JOURNAL OF NANO- AND ELECTRONIC PHYSICS
Vol. **17** No 6, 06036(9pp) (2025)

ЖУРНАЛ НАНО- ТА ЕЛЕКТРОННОЇ ФІЗИКИ
Том **17** № 6, 06036(9cc) (2025)

REGULAR ARTICLE

Optical Phenomena in Spherical Metallic Nanoparticles. Nonlocal Theory

R.Yu. Korolkov*, O.Yu. Berezhnyi

Zaporizhzhia Polytechnic National University, 69011, Zaporizhzhia, Ukraine

(Received 19 July 2025; revised manuscript received 14 December 2025; published online 19 December 2025)

An influence of the nonlocal phenomena on the plasmonic properties of the metallic nanoparticles is investigated in the work. The mathematical model for determining the frequency dependences of such optical characteristics as dielectric function, polarizability, absorption and scattering cross-sections is proposed. The relation for the size dependence of the frequencies of the nonlocal multipole surface plasmonic resonances is obtained. It is shown that in the infrared frequency region the difference between the Drude theory and the nonlocal theory is very significant, while in the optical region of the spectrum the results of the calculations of the corresponding dielectric functions are practically identical. It is found that in both Drude and nonlocal theories, the change in the size of the nanoparticles affects only the width of the spectral line and not the magnitude of the frequency of nonlocal (or local) surface plasmonic resonances. The results of the calculations indicate the presence of the blue shift of the maxima of the imaginary part of the nonlocal polarizability with increasing order of multipolarity and the maximum of the imaginary part of the nonlocal dipole polarizability with respect to the maximum of the imaginary part of the local polarizability. It is shown that for the relatively small nanoparticles the maximum absorption and scattering cross-sections are of the same order, whereas with the increasing radius the scattering processes begin to dominate over the absorption processes. The complete analogy in the behavior of the frequency dependence curves of the imaginary part of the polarizability and absorption cross-section is demonstrated, which is explained by the linear coupling of these optical characteristics. The significant influence on the character of the frequency dependences of the absorption cross-section of both the material properties of the nanoparticles and the properties of the surrounding dielectric was established. It is shown that the behavior of the surface plasmonic resonance frequencies in Drude theory and nonlocal theory has both similarities and differences. In particular, with increasing multipolarity both theories predict the increase of this frequency. At the same time at the same multipolarity the resonance frequency according to the Drude theory does not depend on the particle radius, whereas according to the nonlocal theory the resonance frequency decreases with increasing of the particle radius.

Keywords: Spherical metallic nanoparticle, Dielectric function, Nonlocal theory, Polarizability, Surface plasmonic resonance, Absorption and Scattering cross-sections.

DOI: 10.21272/jnep.17(6).06036 PACS numbers: 78.67. – n, 78.67.Bf, 78.20.Ci

1. INTRODUCTION

Metallic nanoparticles form a vast family of objects of increasing diversity, complexity and technological importance due to their unique optical properties. The plasmonic nanoparticles exhibit hypersensitivity to the environment, where interactions with molecules and assemblies of molecules in their neighborhood usually affect the particle properties in the significant and easily observable way. The interaction of plasmons of neighboring nanoparticles or hybridization of two plasmons of the same particle provides practical ways to rationally design of the nanoscale objects with new plasmonic properties [1-5]. An influence of the surrounding dielectric environment [6, 7] also changes the plasmonic properties of the nanoparticle [3, 4, 8, 9]. This effect is of significant interest for the development of the ultra-sensitive sensors on localized surface plasmonic resonance (SPR) capable of eventually detecting single molecular binding events or substances of ultra-low concentrations [10, 11]. In fact, the ease with which the properties of surface plasmons depend on the local environment of the nanoparticles has made accurate measurements of their fundamental characteristics a serious problem that requires serious research efforts. Therefore, the study of plasmonic phenomena in isolated nanoparticles has become the main experimental focus and has made significant progress in understanding the phenomenon of the surface plasmonic resonance in the nanostructures of the different dimensions [4, 13]. For example, in dark-field microspectroscopy, individual nanoparticles are dispersed on the dielectric substrate, where they are then examined using ultraviolet and optical spectroscopy. Combining these local optical measurements with an accurate nanoscale image of the isolated nanostructure (for example, scanning electron microscopy) allows us to associate the plasmonic properties of the specific nanoparticles and their complexes to their geometry. This makes possible the quantitative comparison of the experimental spec-

---

* Correspondence e-mail: romankor@zp.edu.ua

Cite this article as: R.Yu. Korolkov et al., *J. Nano- Electron. Phys.* 17 No 6, 06036 (2025) https://doi.org/10.21272/jnep.17(6).06036

tra and theoretical calculations of their surface electromagnetic modes.

The optical properties of the isolated metallic nanoparticles of different geometries are well described within the framework of quasi-static theory, since their sizes are significantly smaller than the light wavelengths [14-16]. The indicated theory is inherently local, since for the dielectric function the Drude model, which takes into account only the time dispersion, is considered to be valid. However, in many practically important cases, such as electromagnetic pairing between the atomic force microscope probe and the surface (substrate), fluorescence and decay of excited molecules in the neighborhood of nanoparticles, hybrid systems "metallic nanoparticle – semiconductor quantum dot", the spatial dispersion of permittivity plays the significant role. It should also be pointed out that in [17] it was established that the error of the quasi-static approximation, especially at frequencies close to the frequency of the surface plasmonic resonance, is significant. The spatial dispersion is taken into account by replacing the local permittivity by the effective permittivity. In turn, the effective permittivity is expressed in terms of the integral that is found analytically only for some dielectric functions that take into account spatial and time dispersion. Most often the relation, obtained in the hydrodynamic approximation, is used as such a dielectric function. At the same time, the above approach does not take into account the relaxation processes in the metallic nanoparticle and, therefore, this approach also does not provide an accurate description of the properties of the above nanoscale objects.

Let us point out that the detailed study of relaxation processes in the spherical metallic nanochalice is presented in [18]. Thus, the size intervals, in which one or another relaxation mechanism plays a predominant role and the values of radii of nanoparticles of different metals at which the effective relaxation rate will be minimal, have been determined. Therefore, the construction of the nonlocal theory to describe the optical properties of spherical metallic nanoparticles taking into account relaxation processes is an actual task.

2. RELAXATION PROCESSES IN NONLOCAL OPTICS OF METALLIC NANOPARTICLES

2.1 Excitation of Plasmons and the Characteristics of the Absorption Processes in Plasmonic Metals

Plasmonic metallic particles are nanostructures that strongly interact with incident electromagnetic radiation. When irradiated by light with the wavelength longer than the particle size, the oscillations of free electrons of the metal are excited in phase with the electric field of the incident light wave (Fig. 1, *a*). The resonance condition is reached when the frequency of photons coincides with the frequency of the oscillation of free electrons. As a result of plasmonic resonance excitation, light energy is localized in the form of enhanced local electric fields near the surface of metallic nanoparticles. The distribution of these localized electric fields is spatially inhomogeneous and reaches the maximum at the surface [19, 20]. In intense near-field regions, known as plasmonic hotspots between two closely spaced nanoparticles, the field intensity can be increased by a factor of $10^4 - 10^6$ [21]. In turn, the enhanced fields stimulate the cascade of events on time scales ranging from femtoseconds (fs) to nanoseconds (ns), leading to energy dissipation through radiative or non-radiative decay, where the latter contributes to the generation of electron-hole pairs (Fig. 1, *b*) [19].

The absorption of light and the subsequent generation of electron-hole pairs can occur in the following four ways (Fig. 1, *c-e*). First, let us consider the zone structure of metal, which has two states with wave vectors $\mathbf{k}_1$ and $\mathbf{k}_2$. In this case, the absorption process requires the defect (imperfection) or phonon to fulfill the law of conservation of momentum. This eventually leads to the generation of the hot electron and the hole by the intrazone transition from the filled s-state below the Fermi level to the non-filled s-state above the Fermi level (Fig. 1, *c*, blue arrows), where the average energy of each carrier is $\hbar\omega / 2$. The nanoparticles with the diameters on the order of tens of nanometers exhibit relaxation rate $10^{13} - 10^{14}$ s^{-1} for this type of excitation [22, 23]. Second, absorption can occur by the direct diagonal process known as Landau damping, where momentum is conserved due to electron-surface collisions (Fig. 1, *c*, red arrow). In this process, the surface plasmon-polariton is characterized by spatial frequencies that are greater than the difference between the wave vectors of the two states ($\Delta\mathbf{k}$). This intrazone transition leads to the formation of hot electron and the hole in the s-zone with average energy $\hbar\omega / 2$, and the excitation rate depends mainly on the size of the nanoparticle as $\gamma \sim \upsilon_{\mathrm{F}} / R$, where υ_{F} is the Fermi electron velocity, and R is the radius of the nanoparticle [19, 24]. Third, the intraband absorption can occur by electron-electron scattering, where the momentum is conserved during reflection, that is, the summation of the reciprocal lattice vector with the result of the addition of two initial wave vectors (Fig. 1, *d*). This leads to the formation of four "hot" carriers from the single photon, rather than two, having the total energy $\hbar\omega$, so that the average energy of each carrier is equal to $\hbar\omega / 4$. This process occurs at the rate $\sim 10^{15} \left(\varepsilon_{\mathrm{ph}} / \varepsilon_{\mathrm{F}}\right)^2$ s^{-1}, where $\varepsilon_{\mathrm{ph}}$ is the photon energy, ε_{F} is Fermi energy [19, 24, 25]. Fourth, interzone excitation can occur from d-zone to s-zone where momentum is conserved (Fig. 1, *e*), and this leads to the higher relaxation rate $\sim 10^{15}$ s^{-1} [23]. The electrons generated from this excitation have low energy because they are generated near the Fermi level. In contrast, high-energy holes are generated in the d-zone.

In order to simplify the description of all four processes, we can say that the generation of the charge carriers by non-radiative decay can occur via intrazone $s-s$-excitation or interzone $d-s$-excitation, where direct interzone excitations with high relaxation rate are usually the pre-dominant way of the decay when they are energetically available [27]. Noble metals, especially Ag, have their own d-zones, located significantly below the Fermi level, so interzone excitations cannot be induced by the visible light. However, Au and Cu have d-zones closer to

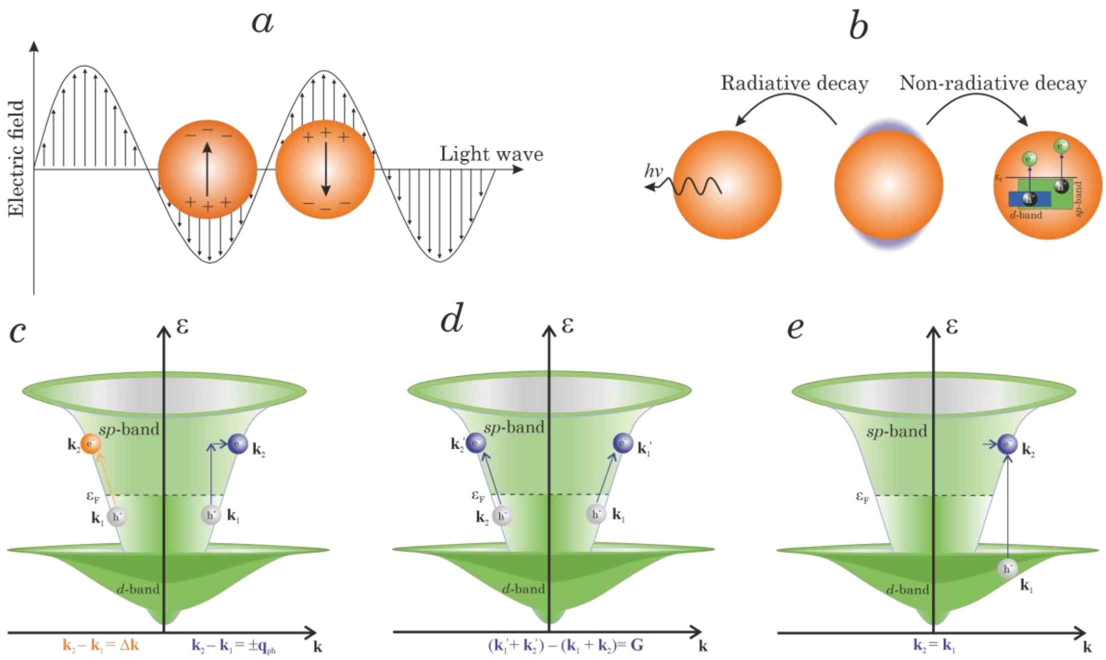

Fig. 1 – The excitation and the decay of plasmons due to the electron excitation [26]: *a* – the interaction between the electromagnetic radiation and the pasmonic metallic nanoparticle and the excitation of the localized SPR; *b* – the dissipation of energy of the local electric fields near the the surface of the metallic nanoparticles due to the radiative or non-radiative decay; *c* – indirect, in-band electron-electron, phonon-assisted (blue arrow) and surface-assisted “diagonal” transitions (orange arrow; *d* – indirect, in-band s-s, electron-electron transition assisted by scattering, where momentum is conserved due to the reflection ; *e* – direct, interzone d-s transition

the Fermi level than Ag; hence, interzone transitions can be induced by the visible light above the certain level. On the contrary, in base metals the d-zone is partially filled and crosses the Fermi level, demonstrating the interzone transition in the whole visible range.

2.2 Mathematical Model

The optical phenomena in spherical metallic nanoparticles, when it is necessary to take into account the spatial dispersion of permittivity, will be described in the framework of the concept of effective permittivity. According to this concept, the expression for multipole polarizability of the metallic nanosphere of the radius R, located in the medium with the permittivity ϵ_{m}, formally coincides with the expression for thr polarizability in the local theory

$$\alpha_l^{\mathrm{NL}}(\omega) = 3V \frac{\epsilon_l^{\mathrm{NL}}(\omega) - \epsilon_{\mathrm{m}}}{\epsilon_l^{\mathrm{NL}}(\omega) + \dfrac{l+1}{l}\epsilon_{\mathrm{m}}}, \tag{1}$$

but with the permittivity, replaced by the effective (nonlocal) permittivity [28, 29]

$$\epsilon_l^{\mathrm{NL}}(\omega, R) = \left\{ \frac{2}{\pi}(2l+1) R \int_0^{\infty} \frac{j_l^2(kR)}{\epsilon(\omega, k)} dk \right\}^{-1}. \tag{2}$$

In formulas (1) and (2) $V = 4\pi R^3/3$ is the volume of the nanoparticle; l is the order of the multipolarity; $j_l(x)$ is the spherical Bessel function of the order l; $\epsilon(\omega, k)$ is the dielectric function, taking into account the spatial dispersion (hydrodynamic model):

$$\epsilon(\omega, k) = \epsilon^{\infty} - \frac{\omega_p^2}{\omega^2 + \mathrm{i}\,\omega\gamma_{\mathrm{eff}} - \beta^2 k^2}. \tag{3}$$

where k is the wave number; $\beta = \upsilon_{\mathrm{F}}\sqrt{3/5}$; ω_p is plasma frequency; ϵ^{∞} is the contribution of the crystal lattice into the dielectric function; γ_{eff} is the effective electron relaxation rate, the additive contribution in which is made by three mechanisms - volume relaxation, surface relaxation and radiation damping

$$\gamma_{\mathrm{eff}} = \gamma_{\mathrm{bulk}} + \gamma_{\mathrm{s}} + \gamma_{\mathrm{rad}}, \tag{4}$$

moreover bulk relaxation rate $\gamma_{\mathrm{bulk}} = \mathrm{const}$ for each metal, and the expressions for the surface relaxation rate γ_{s} and radiation damping rate γ_{rad} have the form [18]

$$\gamma_{\mathrm{s}} = \mathscr{A}(\omega, R)\frac{\upsilon_{\mathrm{F}}}{R}; \tag{5}$$

$$\gamma_{\mathrm{rad}} = \frac{V}{6\pi}\sqrt{\frac{\epsilon^{\infty} + 2\epsilon_{\mathrm{m}}}{\epsilon_{\mathrm{m}}}}\left(\frac{\omega_p}{c}\right)^3 \mathscr{A}(\omega, R)\frac{\upsilon_{\mathrm{F}}}{R}, \tag{6}$$

and the effective parameter, which describes the degree of the coherence loss under the electron scattering on the surface

$$\mathscr{A}\left(\omega, R\right)=\frac{3}{4}\frac{1}{\epsilon^{\infty}+2\epsilon_{\mathrm{m}}}\left(\frac{\omega_p}{\omega}\right)^2 \times \\ \times\left[1-\frac{2\nu_s}{\omega}\sin\frac{\omega}{\nu_s}+\frac{2\nu_s^2}{\omega^2}\left(1-\cos\frac{\omega}{\nu_s}\right)\right], \qquad (7)$$

$\nu_s = \upsilon_{\mathrm{F}}/2R$ is the frequency of the individual oscillations of electrons.

Calculating improper integral in (2), taking into account the expression (3), we obtain

$$\epsilon_l^{\mathrm{NL}}\left(\omega\right)=\left\{\frac{1}{\epsilon^{\mathrm{D}}\left(\omega\right)}+\frac{2l+1}{\epsilon^{\infty}}\left(\frac{\omega_p R}{\beta u}\right)^2 I_{l+\frac{1}{2}}\left(u\right)K_{l+\frac{1}{2}}\left(u\right)\right\}^{-1}, \qquad (8)$$

where $I_\nu\left(x\right)$, $K_\nu\left(x\right)$ are Infeld and McDonald functions of the order ν,

$$u=\frac{R}{\beta}\sqrt{\frac{\omega_p^2}{\epsilon^{\infty}}-\omega\left(\omega+\mathrm{i}\gamma_{\mathrm{eff}}\right)},$$

and Drude (local) dielectric function

$$\epsilon^{\mathrm{D}}\left(\omega\right)=\epsilon^{\infty}-\frac{\omega_p^2}{\omega\left(\omega+\mathrm{i}\,\gamma_{\mathrm{eff}}\right)}. \qquad (9)$$

The important optical characteristics of the metallic nanoparticles are their absorption and scattering cross-sections, determined by the following relations

$$C_{\mathrm{abs}}=\frac{\omega}{c}\sqrt{\epsilon_{\mathrm{m}}}\,\mathrm{Im}\,\alpha_l^{\mathrm{NL}} \qquad (10)$$

$$C_{\mathrm{sca}}=\frac{1}{6\pi}\frac{\omega^4}{c^4}\epsilon_{\mathrm{m}}^2\left|\alpha_l^{\mathrm{NL}}\right|^2. \qquad (11)$$

Further the formulas (1), (8) – (11) taking into account the expressions (4) – (7) are used for the calculations.

3. RESULTS OF THE CALCULATIONS AND THEIR DISCUSSION

The frequency dependences of the dielectric function, polarizability, and absorption and scattering cross-sections were calculated for the spherical nanoparticles of the different metals and the different radii. The parameters of metals, required for the calculations are given in Table 1

Table 1 – The parameters of metals (a_0 is the Bohr radius) (see, for example, [18, 30] and references therein)

Metals	Value				
	$r_s\,/\,a_0$	$m^*\,/\,m_e$	ϵ^{∞}	$\hbar\omega_p$, eV	$\hbar\gamma_{\mathrm{bulk}}$, eV
Cu	2.11	1.49	12.03	12.6	0.024
Au	3.01	0.99	9.84	9.07	0.023
Ag	3.02	0.96	3.7	9.17	0.016
Pt	3.27	0.54	4.42	15.2	0.069
Pd	4.00	0.37	2.52	9.7	0.091

The comparison of the frequency dependencies for the real and imaginary parts of the local (Drude) and nonlocal dielectric functions for the nanoparticles Ag with $R = 10$ nm in Teflon are presented in Fig. 2. Let us point out that the curves $\mathrm{Im}\,\epsilon^{\mathrm{D}}\left(\omega\right)$ and $\mathrm{Im}\,\epsilon_1^{\mathrm{NL}}\left(\omega\right)$ are qualitatively similar and practically do not differ quantitatively in the optical frequency range. The quantitative differences of the indicated curves are noticeable only in the range $0.7\text{ eV} < \hbar\omega < 1.5\text{ eV}$, at the same time the inequality $\mathrm{Im}\,\epsilon_1^{\mathrm{NL}} > \mathrm{Im}\,\epsilon^{\mathrm{D}}$ is always true, and $\max\left\{\mathrm{Im}\,\epsilon_1^{\mathrm{NL}}\right\}$ is reached at great frequencies in comparison with $\max\left\{\mathrm{Im}\,\epsilon^{\mathrm{D}}\right\}$. The latter facts indicate that in the indicated frequency range (since the imaginary part of the dielectric function is responsible for the absorption) the nonlocal theory predicts the more substantial absorption than the Drude theory, and the absorption will be maximized at the higher frequency. Regarding the real part of the dielectric function, it should be pointed out that, like the imaginary parts at $\hbar\omega > 1.5\text{ eV}$, the real parts of the nonlocal and Drude dielectric functions practically coincide, whereas at $\hbar\omega < 1.5\text{ eV}$ the behavior of the curves $\mathrm{Re}\,\epsilon_1^{\mathrm{NL}}$ and $\mathrm{Re}\,\epsilon^{\mathrm{D}}$ are essentially different. Thus, the real part of the nonlocal dielectric function at $\hbar\omega_0 \approx 0.8\text{ eV}$ has the maximum, which the curves $\mathrm{Re}\,\epsilon^{\mathrm{D}}\left(\omega\right)$ do not have. It should also be pointed out that all curves, shown in Fig. 2, experience small-scale oscillations at $\hbar\omega < 1.0\text{ eV}$, that is, in the near-infrared region of the spectrum, which is explained by the manifestation of the classical size effects.

The frequency dependences of the real and imaginary parts of the nonlocal dielectric function for Ag particles of the different sizes in Teflon are shown in Fig. 3. Let us point out that the extrema (maxima and minima of the real and maxima of the imaginary parts) of the dielectric function shift to the region of high frequencies when the radius of the nanoparticles decreases. Such behavior of the extrema of the real and imaginary parts of the nonlocal dielectric function is similar to the behavior of $\max\left\{\mathrm{Re}\,\epsilon^{\mathrm{D}}\right\}$, $\min\left\{\mathrm{Re}\,\epsilon^{\mathrm{D}}\right\}$ and $\max\left\{\mathrm{Im}\,\epsilon^{\mathrm{D}}\right\}$, and is associated with the decrease in the relaxation rate with increasing radius of the spherical nanoparticles up to the radius corresponding to $\gamma_{\mathrm{eff}}^{\min}$ for the given material [18].

The frequency dependences of the real and imaginary parts, as well as the modulus of the nonlocal dipole polarizability of silver nanoparticles of the different radii in Teflon are demonstrated in Fig. 3. The calculation results indicate the weak influence of the nanoparticle size on the spectral position of $\max\left\{\mathrm{Im}\,\alpha_1^{\mathrm{NL}}\right\}$ and, consequently, on the frequency of the surface plasmonic resonance. At the same time, as the radius of the nanoparticle decreases, the effective relaxation rate increases and, consequently, the width of the resonance line increases. In addition, the curves $\mathrm{Im}\,\alpha_1^{\mathrm{NL}}\left(\omega\right)$ in the infrared region of the spectrum also show small-scale oscillations due to the manifestation of classical size effects.

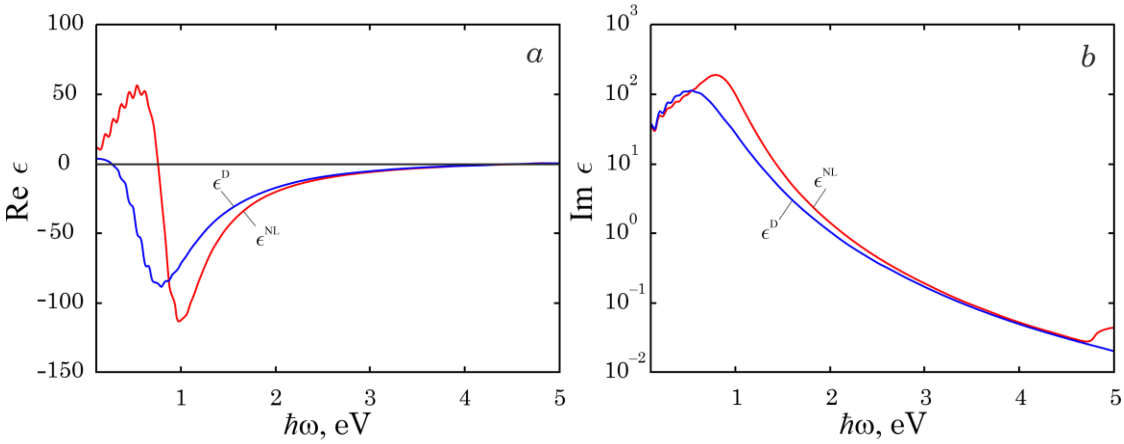

Fig. 2 – The comparison of the frequency dependencies for the real (*a*) and imaginary (*b*) parts of Drude and nonlocal dielectric functions for the nanoparticles Ag with $R = 10$ nm in Teflon

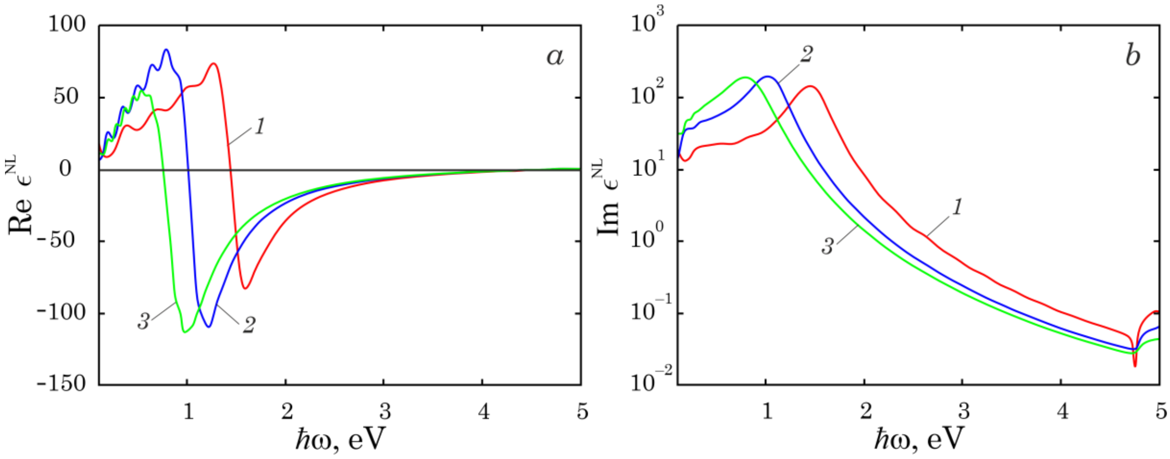

Fig. 3 – The frequency dependencies for the real (*a*) and imaginary (*b*) parts of the nonlocal dielectric function for the nanoparticles Ag of the different radius in Teflon: *1* – $R = 10$ nm; *2* – $R = 20$ nm; *3* – $R = 35$ nm

Concerning the frequency dependences of the real and imaginary parts, as well as the moduli of the nonlocal multipole polarizabilities (Fig. 5), we note the following. All the above curves for the different multipolarities are qualitatively similar, but with increasing multipolarity there is the shift of the curves towards higher frequencies. Thus, with increasing the plasmonic mode number (multipolarity) there is the "blue" shift of $\max\left\{\mathrm{Im}\,\alpha_l^{\mathrm{NL}}\right\}$, and hence the frequency of multipole surface plasmonic resonances grows with increasing the plasmonic mode number.

The comparison of the frequency dependences of the real and imaginary parts, as well as the modulus of the dipole local and nonlocal polarizabilities is presented in Fig. 6. The results of the calculations for these two cases are qualitatively similar and quantitatively close, and the difference consists in the presence of small shifts of $\max\left\{\mathrm{Re}\,\alpha_1^{\mathrm{NL}}\right\}$, $\min\left\{\mathrm{Re}\,\alpha_1^{\mathrm{NL}}\right\}$, $\max\left\{\mathrm{Im}\,\alpha_1^{\mathrm{NL}}\right\}$, $\max\left|\alpha_1^{\mathrm{NL}}\right|$ into the region of greater frequencies. Thus, the frequency of the dipole surface plasmonic resonance, predicted by the nonlocal theory, corresponding to the spectral position of $\max\left\{\mathrm{Im}\,\alpha_1^{\mathrm{NL}}\right\}$, is slightly greater than the same frequency obtained in the local theory.

The frequency dependences of the absorption and scattering cross-sections for Ag nanoparticles of the different radius in Teflon are shown in Fig. 7. It should be pointed out that at relatively small radii (10 and 20 nm) the cross-sections are of one order of magnitude, whereas for relatively large nanoparticles ($R = 35$ nm) the scattering cross-section is an order of magnitude greater than the absorption cross-section. This is consistent with the fact that the role of the scattering processes increases with increasing size of the nanostructures (see, for example, [18]).

The frequency dependences of the absorption cross-sections under the excitation of the plasmonic modes of the different multipolarities for Ag nanoparticles, as well as under the excitation of the dipole mode for Ag particles in different media and for the particles of different metals in Teflon are given in Fig. 8.

The results of the calculations show that $\max\left\{C_{\mathrm{abs}}\right\}$ shift to the region of large frequencies, which is explained by the fact that $C_{\mathrm{abs}} \sim \mathrm{Im}\,\alpha_l^{\mathrm{NL}}$ and therefore there is an analogy in the behavior of the frequency dependence curves of these characteristics. In turn, the position of $\max\left\{C_{\mathrm{abs}}\right\}$ under the excitation of the dipole modes in the particles of different metals differs significantly due to the difference in their optical properties. The influence of the dielectric, surrounding the nanoparticle, is also significant and the maximum of the absorption cross-section shifts to the region of smaller frequencies with increasing permittivity in the sequence $\mathrm{Air} \to \mathrm{CaF_2} \to \mathrm{Teflon} \to \mathrm{Al_2O_3} \to \mathrm{C_{60}}$.

The frequencies of the surface plasmonic resonance can be found from the condition that the real part of the denominator of the expression (1) is equal to zero

$$\operatorname{Re}\epsilon_l^{\mathrm{NL}}(\omega) = -\frac{l+1}{l}\epsilon_{\mathrm{m}}, \qquad (12)$$

where $\operatorname{Re}\epsilon_l^{\mathrm{NL}}$ is the real part of the right-hand side in the expression (8).

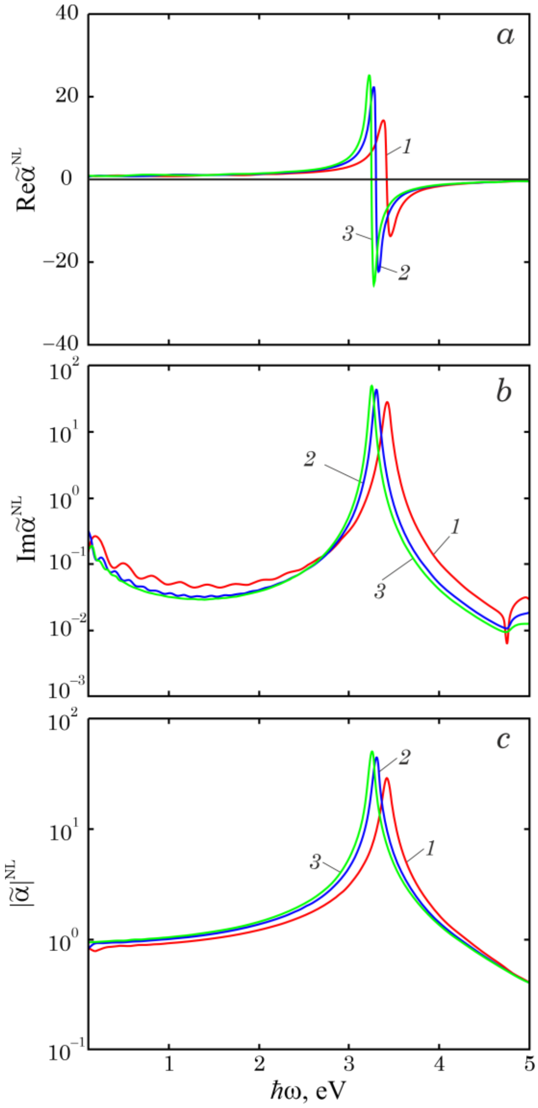

Fig. 4 – The frequency dependencies for the real (*a*) and imaginary (*b*) parts, and the module (*c*) of the nonlocal dipole polarizability of the nanoparticles of silver with the different radius in Teflon: *1* – $R = 10$ nm; *2* – $R = 20$ nm; *3* – $R = 35$ nm

The results of calculations of the surface plasmonic resonance frequencies for Ag and Au nanoparticles of the different radii in Teflon are given in Table 2. According to the results, we can conclude that, in contrast to the classical case, when the frequency of SPR grows with increasing multipolarity order and does not change with increasing particle radius, in the nonlocal theory the frequency of SPR grows with increasing multipolarity order and for the particular value of the multipolarity order decreases slightly with increasing particle size.

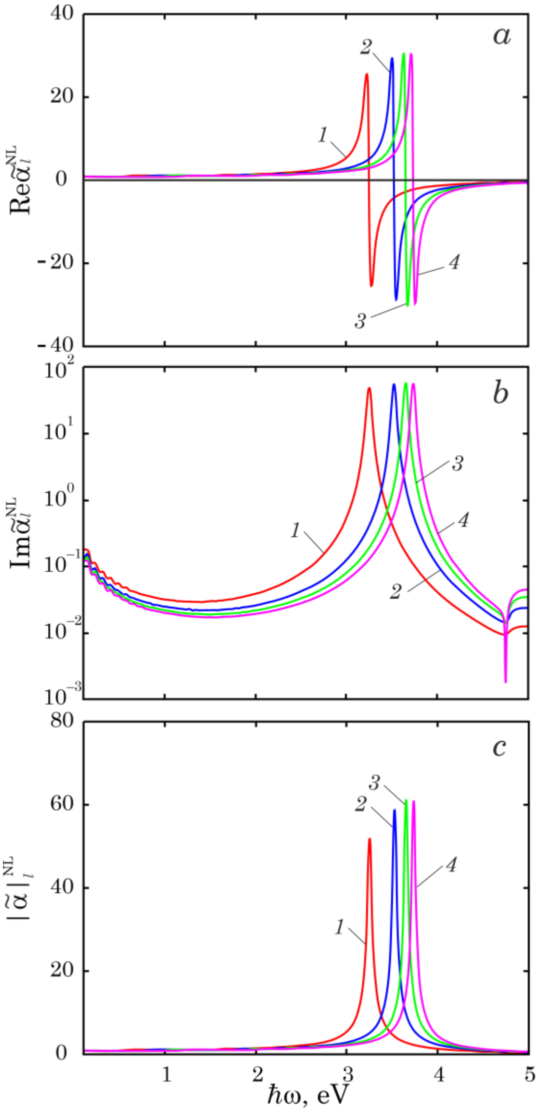

Fig. 5 – The frequency dependencies for the real (*a*) and imaginary (*b*) parts, and the module (*c*) of the nonlocal multipole polarizabilities of the silver nanoparticles with $R = 10$ nm in Teflon: *1* – $l = 1$; *2* – $l = 2$; *3* – $l = 3$; *4* – $l = 4$.

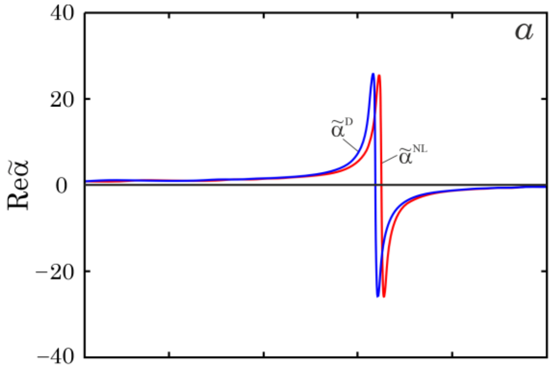

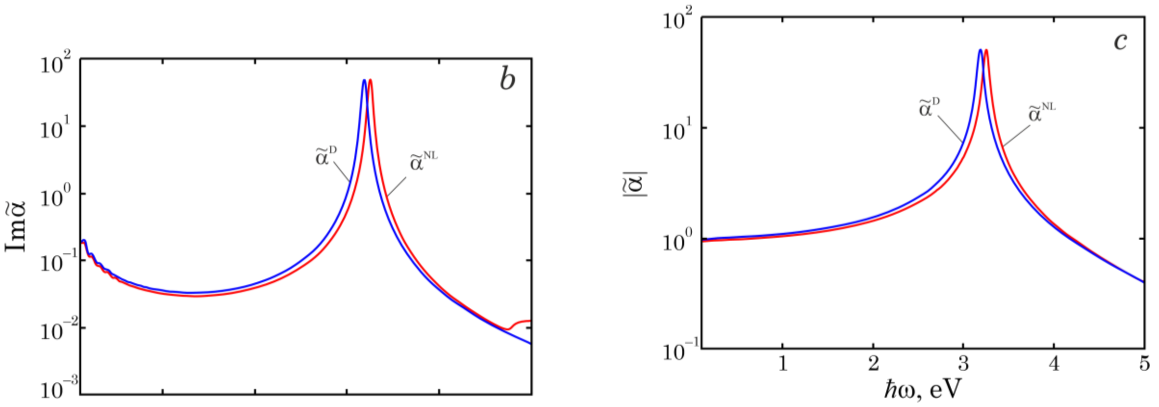

Fig. 6 – The comparison of the frequency dependencies for the real (*a*) and imaginary (*b*) parts and the module (*c*) of the dipole local and nonlocal polarizabilities for the nanoparticles of silver with $R = 10$ nm in Teflon

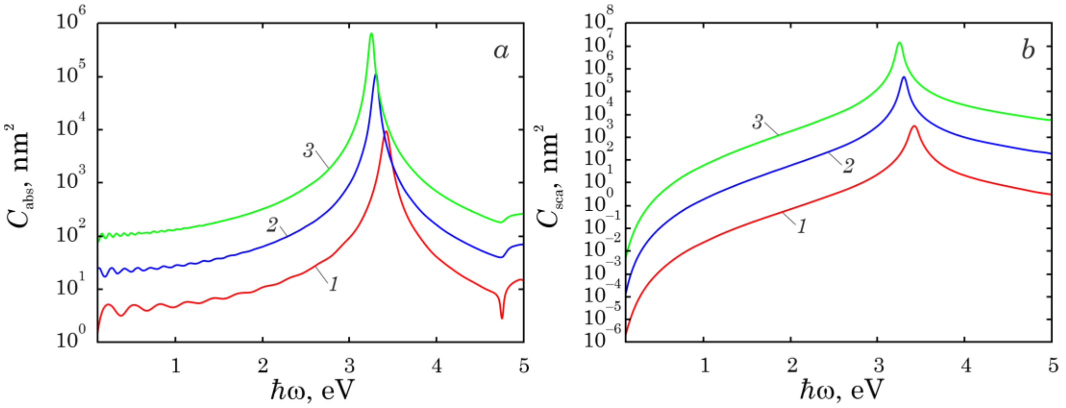

Fig. 7 – The frequency dependencies of the absorption cross-section (*a*) and scattering cross-section (*b*) for the nanoparticles Ag of the different radius in Teflon :*1* – $R = 10$ nm ; *2* – $R = 20$ nm ; *3* – $R = 35$ nm

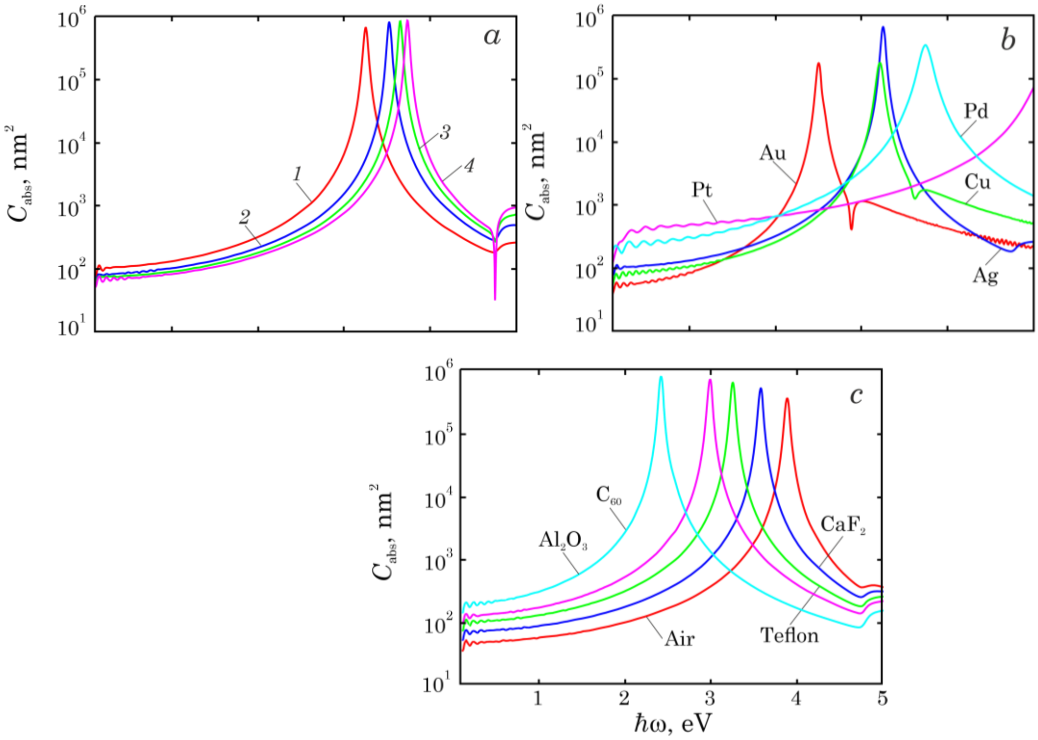

Fig. 8 – The frequency dependencies of the absorption cross-sections under the excitation of the plasmonic modes of the different multipolarity in the nanoparticles Ag in Teflon (*a*): *1* – $l = 1$; *2* – $l = 2$; *3* – $l = 3$; *4* – $l = 4$; dipole plasmonic modes in the nanoparticles of different metals in Teflon (*b*) and dipole plasmonic modes in the nanoparticles Ag, in the different dielectrics (*c*) when the radius of the nanoparticles is $R = 10$ nm

Table 2 – The frequencies of multipole SPR for the spherical metallic nanoparticles Ag and Au of the different radius in Teflon

Ag								
R, nm	$l = 1$		$l = 2$		$l = 3$		$l = 4$	
	ω_{sp}^{cl}, eV	ω_{sp}^{*}, eV	ω_{sp}^{cl}, eV	ω_{sp}^{*}, eV	ω_{sp}^{cl}, eV	ω_{sp}^{*}, eV	ω_{sp}^{cl}, eV	ω_{sp}^{*}, eV
10	3.181	3.197	3.428	3.208	3.524	3.218	3.575	3.228
15	3.181	3.192	3.428	3.199	3.524	3.206	3.575	3.213
20	3.181	3.189	3.428	3.195	3.524	3.200	3.575	3.205
25	3.181	3.188	3.428	3.192	3.524	3.196	3.575	3.201
30	3.181	3.187	3.428	3.190	3.524	3.194	3.575	3.197
35	3.181	3.186	3.428	3.189	3.524	3.192	3.575	3.195
40	3.181	3.185	3.428	3.188	3.524	3.191	3.575	3.193
45	3.181	3.185	3.428	3.187	3.524	3.190	3.575	3.192
50	3.181	3.185	3.428	3.187	3.524	3.189	3.575	3.191
Au								
R, nm	$l = 1$		$l = 2$		$l = 3$		$l = 4$	
	ω_{sp}^{cl}, eV	ω_{sp}^{*}, eV	ω_{sp}^{cl}, eV	ω_{sp}^{*}, eV	ω_{sp}^{cl}, eV	ω_{sp}^{*}, eV	ω_{sp}^{cl}, eV	ω_{sp}^{*}, eV
10	2.387	2.389	2.488	2.391	2.525	2.392	2.544	2.394
15	2.387	2.389	2.488	2.390	2.525	2.391	2.544	2.392
20	2.387	2.388	2.488	2.389	2.525	2.390	2.544	2.391
25	2.387	2.388	2.488	2.389	2.525	2.389	2.544	2.390
30	2.387	2.388	2.488	2.388	2.525	2.389	2.544	2.389
35	2.387	2.388	2.488	2.388	2.525	2.389	2.544	2.389
40	2.387	2.388	2.488	2.388	2.525	2.388	2.544	2.389
45	2.387	2.388	2.488	2.388	2.525	2.388	2.544	2.389
50	2.387	2.388	2.488	2.388	2.525	2.388	2.544	2.388

For both Ag and Au particles, this reduction is more significant for the higher multipole modes, and the comparison of the results for the particles of these metals indicates the more significant reduction of these frequencies for Ag particles than for Au particles. This difference is explained by the difference in the position of the *d*-zones of these metals relative to the Fermi level.

4. CONCLUSIONS

The expressions for the dielectric function, polarizability, and absorption and scattering cross-sections of the spherical metallic nanoparticles taking into account nonlocal phenomena, as well as the size dependences of the frequencies of the nonlocal multipole surface plasmonic resonances have been obtained.

It has been found that the curves of the frequency dependences of the real and imaginary parts of the dielectric function in the local and nonlocal theories for the optical frequency range practically coincide, whereas in the infrared frequency range the differences between them are significant.

It has been shown that the character of the shifts of the maxima of the imaginary part of the polarizability and the changes in the width of the spectral line for Drude theory and nonlocal theory are the same. Thus, when the order of the multipolarity increases, the indicated maxima shift to the region of higher frequencies, while when the nanoparticle radius increases, the spectral line width increases, and the positions of the maxima do not change in the local theory and change weakly in the nonlocal theory.

The presence of small-scale oscillations on the curves of frequency dependences of the real (imaginary) part of the dielectric function (polarizability) associated with the manifestation of the classical size effect in the infrared frequency region has been demonstrated.

It has been found that for the relatively large nanoparticles the scattering cross-section is an order of magnitude greater than the absorption cross-section, whereas for the particles of the relatively small radius these values are of the same order of magnitude.

It has been shown that the nature of the frequency dependence of the absorption cross-section depends significantly on the material of the nanoparticles and the surrounding dielectric due to the difference in their optical and electrophysical properties.

For the nonlocal theory, the slight decrease in the surface plasmonic resonance frequencies of the arbitrary multipolarity with increasing nanoparticle radius has been predicted.

REFERENCES

1. E. Prodan, C. Radloff, N.J. Halas, P. Nordlander, *Science* **302**, 419 (2003).
2. H. Wang, D.W. Brandl, P. Nordlander, N.J. Halas, *Acc. Chem. Res.* **40**, 53 (2007).
3. N.L. Dmitruk, S.Z. Malynych, I.E. Moroz, *J. Nano- Electron. Phys.* **5** No 3, 03031 (2013).
4. A.O. Koval, A.V. Korotun, Yu.A. Kunytskyi, V.A. Tatarenko, I.M. Titov, *Electrodynamics of Plasmon Effects in Nanomaterials* (Kyiv: Naukova Dumka: 2021) [in Ukrainian].
5. Y. Yang, Y. Jeon, Z. Dong, J.K.W. Yang, M.H. Moghaddam, D.-S. Kim, D.K. Oh, J. Lee, M. Hentschel, H. Giessen, D. Kang, G. Kim, T. Tanaka, Y. Zhao, J. Bürger, S.A. Maier, H. Ren, W. Jung, M. Choi, G. Bae, H. Chen, S. Jeon, J. Kim, E. Lee, H. Kang, Y. Park, D.D. Nguyen, I. Kim, P. Cencillo-Abad, D. Chanda, X. Jing, N. Liu, I.V. Martynenko, T. Liedl, Y. Kwak, J.-M. Nam, S.-M. Park, T.W. Odom, H.-E. Lee, R.M. Kim, K.T. Nam, H. Kwon, H.-H. Jeong, P. Fischer, J. Yoon, S.-H. Kim, S. Shim, D. Lee, L.A. Pérez, X. Qi,

A. Mihi, H. Keum, M. Shim, S. Kim, H. Jang, Y.S. Jung, C. Rossner, T.A.F. König, A. Fery, Z. Li, K. Aydin, C.A. Mirkin, J. Seong, N. Jeon, Z. Xu, T. Gu, J. Hu, H. Kwon, H. Jung, H. Alijani, I. Aharonovich, J. Kim, J. Rho, *ACS Nano* **19** No13, 12491 (2025).

6. L.J. Sherry, S.H. Chang, G.C. Schatz, R.P. Van Duyne, B.J. Wiley, Y. Xia, *Nano Lett.* **5**, 2034 (2005).
7. F. Tam, C.E. Moran, N.J. Halas, *J. Phys. Chem. B* **108**, 17290 (2004).
8. A. Dmitriev, C. Hägglund, S. Chen, H. Fredriksson, T. Pakizeh, M. Käll, D.S. Sutherland, *Nano Lett.* **8**, 3893 (2008).
9. V. Myroshnychenko, J. Rodríguez-Fernández, I. Pastoriza-Santos, A.M. Funston, C. Novo, P. Mulvaney, L.M. Liz-Marzán, F.J. García de Abajo, *Chem. Soc. Rev.* **37**, 1792 (2008).
10. T. Sannomiya, C. Hafner, J. Voros, *Nano Lett.* **8**, 3450 (2008).
11. K.M. Mayer, S. Lee, H. Liao, B.C. Rostro, A. Fuentes, P.T. Scully, C.L. Nehl, J.H. Hafner, *ACS Nano* **2**, 687 (2008).
12. M.B. Almeida, C.M.R. Galdiano, F.S.R.D. Silva Benvenuto, E. Carrilho, L.C. Brazaca, *ACS Appl. Mater. Interf.* **16** No 49, 67054 (2024).
13. C. Sonnichsen, T. Franzl, T. Wilk, G. von Plessen, J. Feldmann, O. Wilson, P. Mulvaney, *Phys. Rev. Lett.* **88**, 077402 (2002).
14. A.V. Korotun, A.A. Koval', V.I. Reva, *J. Appl. Spectrosc.* **86** No 4, 606 (2019).
15. A.V. Korotun, N.I. Pavlishche, *Opt. Spectrosc.* **130** No 4, 269 (2022).
16. A.V. Korotun, Ya.V. Karandas, V.I. Reva, *Ukr. J. Phys.* **67** No 12, 849 (2022).
17. V.V. Datsyuk, *Ukr. J. Phys.* **56**, 122 (2011).
18. A.V. Korotun, H.V. Moroz, R.Yu. Korolkov, *Funct. Mater.* **31** No 1, 119 (2024).
19. N.J. Halas, S. Lal, W.-S. Chang, S. Link, P. Nordlander, *Chem. Rev.* **111**, 3913 (2011).
20. E. Hao, G.C. Schatz, *J. Chem. Phys.* **120**, 357 (2004).
21. S. Linic, P. Christopher, D.B. Ingram, *Nat. Mater.* **10**, 911 (2011).
22. G.V. Hartland, *Chem. Rev.* **111**, 3858 (2011).
23. J.B. Khurgin, *Nat. Nanotechnol.* **10** No 1, 2 (2015).
24. S. Linic, S. Chavez, R. Elias, *Nat. Mater.* **20**, 916 (2021).
25. F. Abeles, *Optical Properties of Solids* (Ed. by F. Abeles) (American Elsevier: 1972).
26. J.B. Khurgin, *Nanophotonics* **9**, 453 (2020).
27. A.M. Brown, R. Sundararaman, P. Narang, W.A. Goddard, H.A. Atwater, *ACS Nano* **10**, 957 (2016).
28. B.B. Dasgupta, R. Fuchs, *Phys. Rev. B* **24**, 554 (1981).
29. R. Fuchs, F. Claro, *Phys. Rev. B* **35**, 3722 (1987).
30. V.I. Reva, M.A. Shvydkyi, R.Yu. Korolkov, A.V. Korotun, E.V. Stegantsev, O.S. Hnatenko, *J. Nano- Electron. Phys.* **17** No 2, 02006 (2025).

Оптичні явища в сферичних металевих наночастинках. Нелокальна теорія

Р.Ю. Корольков, О.Ю. Бережний

Національний університет «Запорізька політехніка», 69011 Запоріжжя, Україна

В роботі досліджено вплив нелокальних явищ на плазмонні властивості металевих наночастинок. Запропоновано математичну модель для визначення частотних залежностей таких оптичних характеристик як діелектрична функція, поляризовність, перерізи поглинання та розсіювання. Отримано співвідношення для розмірної залежності частот нелокальних мультипольних поверхневих плазмонних резонансів. Показано, що в інфрачервоній області частот відмінності між теорією Друде і нелокальною теорією є досить суттєвими, у той час як в оптичній області спектра результати розрахунків, відповідних діелектричних функцій практично ідентичні. Встановлено, що як у теорії Друде, так і в нелокальній теорії зміна розміру наночастинок впливає лише на ширину спектральної лінії, а не на величину частоти нелокальних (або локальних) поверхневих плазмонних резонансів. Результати розрахунків свідчать про наявність синього зсуву максимумів уявної частини нелокальної поляризовності зі збільшенням порядку мультипольності і максимуму уявної частини нелокальної дипольної поляризовності відносно максимуму уявної частини локальної поляризовності. Показано, що для відносно малих наночастинок максимальні перерізи поглинання та розсіювання мають один порядок, тоді як зі збільшенням радіусу процеси розсіювання починають переважати над процесами поглинання. Продемонстровано повну аналогію в поведінці кривих частотних залежностей уявної частини поляризовності і перерізу поглинання, що пояснюється лінійним зв'язком вказаних оптичних характеристик. Встановлено суттєвий вплив на характер частотних залежностей перерізу поглинання як властивостей матеріалу наночастинок, так і властивостей навколишнього діелектрика. Показано, що поведінка частот поверхневого плазмонного резонансу теорії Друде і нелокальної теорії має як подібності, так і відмінності. Зокрема, зі зростанням мультипольності обидві теорії передбачають збільшення цієї частоти. У той же час за однакової мультипольності резонансна частота за теорією Друде не залежить від радіусу частинки, тоді як за нелокальною теорією резонансна частота зменшується зі збільшенням радіусу частинки.

Ключові слова: Сферична металева наночастинка, Діелектрична функція, Нелокальна теорія, Поляризовність, Поверхневий плазмонний резонанс, Перерізи поглинання та розсіювання.